A computational and experimental investigation into the effects of debris on an inverted double wing in ground effect

Abstract

Cars in several motor sports series, such as Formula 1, make use of multi-element front wings to provide downforce. These wings also provide onset flows to other surfaces that generate downforce. These elements are highly loaded to maximise their performance and are generally operating close to stall. Rubber debris, often known as marbles, created from the high slip experienced by the soft compound tyres can become lodged in the multiple elements of a front wing. This will lead to a reduction in the effectiveness of the wing over the course of a race. This work will study the effect of such debris, both experimentally and numerically, on an inverted double element wing in ground effect at representative Reynolds numbers. The wing was mounted at two different ride heights above a fixed false-floor in the Loughborough University wind tunnel and the effect of debris blockage modelled by closing sections of the gap between elements with tape. The reduction in downforce compared to the clean wing was measured and the sensitivity to the size and position of the blockage studied. It was found that debris near the centre of the element has a greater impact. CFD simulations were also carried out that were able to correctly predict the trend of downforce with blockage position. The CFD was also used to computationally remove the effects of the tunnel. This confirmed the result seen in experiment that the blockage has more effect on a more highly loaded wing.

Introduction

High levels of aerodynamic downforce are essential to the operation of modern racing cars in several motor sports series, such as Formula 1, as it is needed to provide the mechanical grip to allow cornering at high speeds [1]. However, the total downforce is not always the driving factor in design; the longitudinal aerodynamic balance of the car plays a significant role in its handling characteristics. Furthermore, the wake of the front wing affects the flow over other parts of the car, such as the leading edge of the floor, that are crucial to generating downforce. Race car wings, particularly those at the front of the car, are operated in close proximity to the ground as this is known to give significantly higher lift coefficients than when operating in freestream conditions due to the 'ground effect' [2] [3] [4]. Front wings are typically made up of multiple elements, as this maximises the downforce produced by a wing that is limited in its physical geometry by technical regulations. Several studies have been conducted into the behaviour of multi-element wings in ground effect. A fixed ground plane study was carried out by Jasinski & Selig [5] that examined the design parameters that would affect the performance of a double element wing operating in ground effect. A similar computational study was conducted by Soso & Wilson [6],

but made use of a moving ground plane. A comprehensive experimental study on a two-element wing was conducted by Zhang and Zerihan [7] who studied the effect of ground clearance and flap deflection. They showed that as the ground clearance is reduced the downforce increases until a critical ground clearance when the downforce reduces rapidly with height due to flow separation. Increasing flap deflection was seen to increase downforce, but due to the increased loading on the wing the loss of downforce due to separation occurs at a higher ground clearance. A further experimental study [8] also showed the importance of considering a finite length three-dimensional wing due to the importance of phenomena such as edge vortices. The ability of steady RANS based CFD methods to predict surface pressures and wake profiles in a 2D, infinite-span, arrangement was assessed in [9]. Good agreement was found for ground clearances above the critical height but it would be expected that 3D effects or separations encountered with higher loading would prove more challenging.

A particular issue for race car wings in ground effect is tyre debris, whereby rubber 'marbles' deposited by degrading tyres onto the surface of the race track become lodged in slot gaps in the front wing. These will affect the aerodynamic performance of the wing, especially if the flow is close to separation in its clean configuration. This is particularly likely in race car applications where to maximise aerodynamic performance the wings are designed to operate as close as possible to the limits of ground clearance and flap angle, for example as observed experimentally in [7]. However front wings rarely operate in perfect conditions, and so there is the need to understand how this can affect the handling of the vehicle. Relatively little work has been published in this area with the most relevant work to be found in studies of the effect of ice accretion on aircraft wings. Bragg et al. summarise the results of several studies [10] and conclude that leading edge build-up has the most severe effect on the wing performance, due to it causing large regions of separation over the wing. Aerofoil performance is also affected by small scale ice accretion; it increases the surface roughness and so trips the boundary layer. The effect of icing on high-lift configuration wings has been investigated by Sang et al. [11], Bidwell [12] and Silva et al. [13]. They all highlighted the critical situation of ice accumulating during hold, resulting in a loss of performance during descent, approach and landing, whilst the high-lift devices are deployed. Silva & Trapp analysed a range of turbulence models to investigate the variation in how they predict the flow around both clean and iced aerofoils [14]. There was poor correlation to experiment force and pressure coefficients, with all turbulence models predicting a lower stall angle and lower $C_{L,max}$. This was due to the over-prediction of the separation bubble, highlighting the challenge of simulating wing performance in compromised configurations.

While ice accretion on wings will typically lead to increased surface roughness or build up on the leading edge, tyre and other track debris can be of a size comparable to the gaps between elements and can lead to localised blocking of this gap. This paper aims to investigate the effect of blocking the gap between main element and flap of a two-element wing in ground effect. An experimental study is carried out using a finite span wing with endplates installed above a false floor in a wind tunnel facility. To obtain well-characterised and reproducible blockages, lengths of tape are used to seal sections of the gap between main element and flap. The influence of the length and position of the blockages are investigated. The effect of the position of the blockage is also investigated using CFD to investigate the ability of steady RANS based methods to predict the effect of blockages and to give some further insight into the flow. The influence of the degree of loading of the clean wing on the effect that debris can cause is also investigated by changing flap angle experimentally and using the CFD to switch from a stationary to a moving ground plane.

Experimental Methodology

Testing was performed in the Loughborough University Wind Tunnel, Figure 1, full details of which can be found in [15]. The freestream turbulence intensity in the middle of an empty test section is approximately 0.2 % and flow uniformity ±0.4 %. The force range and accuracy of the balance are shown in Table 1.
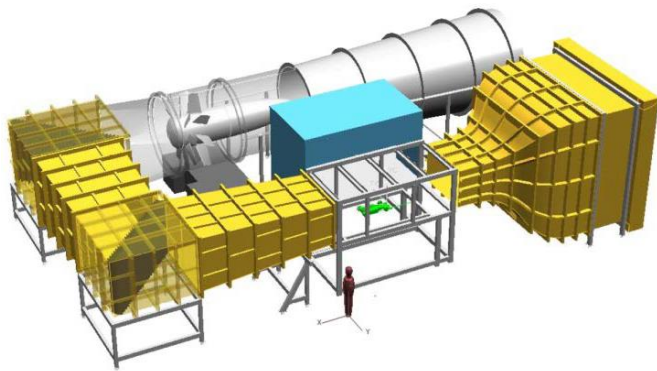

Figure 1. The Loughborough University Wind Tunnel

Table 1. Accuracy of force measurements from the under-floor balance

Component	Force Range (N)	Accuracy (% of full scale)
Drag, C_d	±120	0.010
Side Force, C_y	±420	0.005
Lift, C_L	±500	0.010

The wind tunnel model consists of a double element wing with a span, b, of 500 mm mounted between two end plates. The main wing element has a NACA4412 aerofoil, with a chord of 200 mm and a second flap element with a chord of 79 mm. The flap overlaps the trailing edge of the main element by 7 mm and the vertical gap between the trailing edge of the main element and the lowest point of the flap is 9 mm. The overall chord length of the two elements combined, c, is 272 mm and this is the value that has been used to calculate non-dimensional parameters. Due to the absence of a

moving ground plane in the wind tunnel facility a false floor, which extends 1170 mm upstream of the wing assembly, was used to reduce the boundary layer growth. The influence of the presence of a stationary ground plane were subsequently investigated using the CFD simulations. Slots in the false floor allow the end plates of the wing assembly to be connected to the underfloor force balance. The wing can be positioned at variable ground clearances; however only results at a ground clearance of $h/c=0.2$ are presented here. The flap can be angled to two different incidences (2º and 20º). The arrangement of the wing and false floor is shown in Figure 2 along with a cross section view of the two elements.
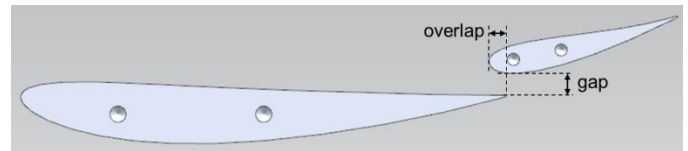

Figure 2. Arrangement of wing and false floor assembly (top), note that the end plates attach to force balance through slots in the false floor. Cross section of two element wing used (bottom) with flap shown in 20º position. Overlap is 7mm and gap is 9mm.

The wind tunnel was run at a working section velocity of 40 m/s, equating to a Re of 7.4 x 10^5 (using the combined chord of the two elements for the characteristic length). A Reynolds number sweep was also included to investigate the sensitivity to variation in Re at this condition; the tunnel was run at velocities between 10 m/s and 40 m/s (in increments of 5 m/s), equating to Re between 1.85×10^5 and 7.40×10^5.

To represent debris blocking the gap between elements tape was used to block part of the gap between the main and flap elements. Two pieces of tape were used for each blockage, one connecting the trailing edge of the main element to the flap and the other connecting the leading edge of the flap to the main element. This method allows the extent of the blocked region to be easily varied and gives a well-defined geometry suitable for comparison with CFD simulations. Two investigations were performed to assess the influence of the extent and position of the blockage. In the first the width of a centrally positioned blockage was varied from 10%, as shown in the photograph in Figure 2, to 100% of the wing span. The investigation into blockage position was initially done using a single piece of tape of width 10% of span moved from mid-span (middle of Figure 3) to the end plate. After this two pieces of tape of 5% span each were placed symmetrically either side of the centre line (bottom of Figure 3) and the gap between them varied to investigate the interaction of two blockages and the influence of the location of a blockage while maintaining a symmetric configuration.
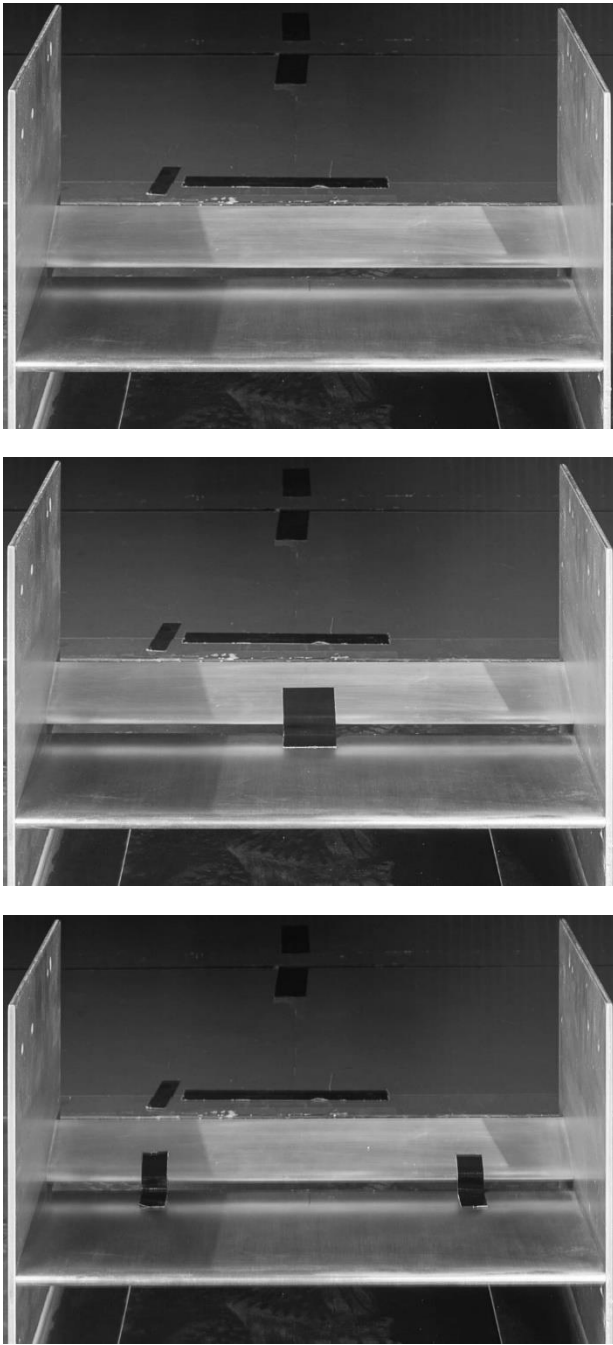
Figure 3. Example tape blockages, from top down: No blockage, 10% central blockage, 10% blockage separated by 30%

Flow visualisation was also obtained to provide an indication of the local flow features present. A mixture of paraffin, titanium di-oxide and oil was used to cover the upper and lower surfaces of each wing, as well as the end plates and the false floor. This was applied using span-wise strokes to ensure that brush strokes could be distinguished from the flow patterns. A mirror was used to capture images of the flow on the suction side of the wing, as attempting to remove the wings from the model would be likely to spoil the flow patterns.

Once these images had been captured, the wings were removed to allow the floor to be photographed.

CFD Methodology

CFD simulations have been carried out for the cases with two 5% span blockages positioned at increasing distances from the centerline. This was done with the twin aims of assessing the ability of typical RANS based method to predict the effect of the debris and to use the simulated results to give further insights into the experimental results. In particular, the CFD can be used to computationally 'remove' the presence of the stationary ground plane and the proximity of the tunnel walls.

Simulations used the Star-CCM+ CFD [16] package and were carried out using a SIMPLE pressure correction solver with constant density operating in steady state mode. A RANS turbulence modelling approach was used with the Menter k-ω-SST model. This model has previously been found by Mahon & Zhang [9] to give accurate results for surface pressure and section forces for a double element aerofoil in ground effect. The SST formulation in Star-CCM+ has an 'All-y+' treatment in which near wall models are applied as appropriate depending on the calculated y+ values. The near wall cell thickness for the wings and endplates was chosen so that a y+ of 1 was achieved across the surface of the whole model to resolve the viscous sub-layer of the boundary layer on the wing. Conversely, the near-wall cell thickness over the walls of the wind tunnel (ceiling, floor and outer wall) was set such that the y+ was 50-60 to reduce the overall cell count.

To compare with experimental results the simulation was setup with the wind tunnel working section as the domain. This has an inlet cross-section of 1920 mm x 1320 mm, which expands to 1940 mm x 1320 mm at the exit with a 3.6 m long working section. To reduce simulation size this domain and the wing assembly are split at mid-span and a symmetry plane used to halve the computational domain. To simulate the false floor that was used in the wind tunnel a portion of the floor boundary, extending 1170 mm upstream of the wing, was set as a no-slip wall. The sections of the floor upstream and downstream of the no-slip floor were set as slip walls as is shown in Figure 4. The wing assembly, roof and sides of the tunnel are no-slip walls. The inlet and outlet boundaries were also extended 50 chord lengths upstream and downstream of the working section with parallel sided sections so that these boundaries do not influence the results. These sections have slip walls to prevent boundary layer development prior to the working section. When simulating the blockage as with the experiment, two pieces of tape were used, one on the leading edge of the flap and one on the trailing edge of the main element. The thickness of the tape was set to 1 mm. Although this is greater than the thickness of the tape used in the experiment, if it was any thinner, the mesh resolution around the tape would have to be excessively fine to capture the geometry. To investigate the influence of the wind tunnel another domain was used in which the side and roof boundaries are moved to 50 chord lengths from the model geometry to approximate freestream conditions. All boundaries other than wing assembly itself are set as slip walls in this case.

The 'trimmer' meshing algorithm was used in Star-CCM+ to generate hexahedral dominant meshes with cut cell and prismatic cells around the model geometry. As mentioned previously, near wall spacing close to the tunnel walls was set to be equivalent to a y+ of 50-60 while that on the model assembly itself was set to be approximately 1. Refinement regions were used around leading and trailing edges of both elements as well as in the wake as can be seen in Figure 4. The final total cell count varied between each condition

(ground height and size of debris), but all meshes consisted of between 5 million and 6 million cells.
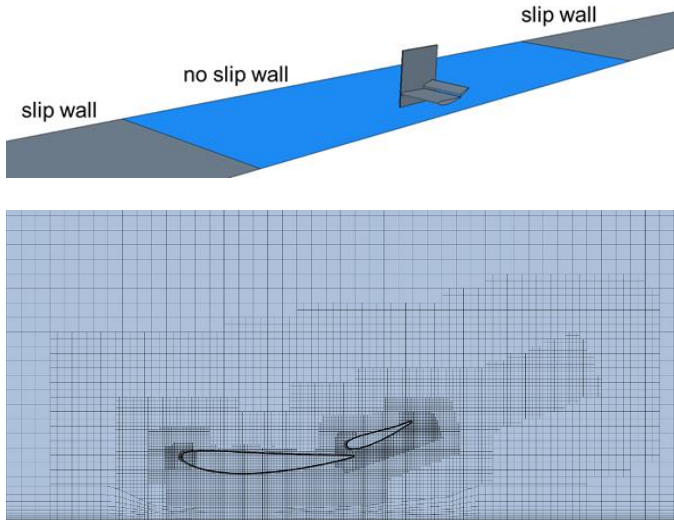

Figure 4. Detail of arrangement of wing and false floor assembly used in CFD for tunnel conditions (top). Note that a half geometry is used to take advantage of the span-wise plane of symmetry. Detail of mesh (bottom) for double element aerofoil with flap angle 20°.

Results

Baseline Results

The experimental force coefficients for the 'clean' wing with two flap angles are shown in Table 2. As expected the increase in flap angle gives an increase in loading. These results are in agreement with previous studies such as those in [7]. The CFD is able to predict the trend of lift and drag with increased flap angle and the absolute agreement with experiment is within approximately 15% for the lift coefficient. As will be shown later there are regions of separated flow present even for those cases with no additional blockage and these present a challenge for steady RANS modelling as used here.

Table 2. Experimental and CFD force coefficient data for wing in 'clean' configuration.

Flap Angle (°)	Exp. Lift Coefficient, C_L	CFD. Lift Coefficient, C_L	Exp. Drag Coefficient, C_D	Exp. Drag Coefficient, C_D
2	-0.844	-0.98	0.0766	0.06
20	-2.05	-1.76	0.196	0.185

Experimental Sensitivity to Reynolds Number

A sweep of Reynolds number was conducted to determine if the performance of a double-element wing in ground effect was still sensitive to changes in Reynolds number at the chosen operating conditions. This investigation was carried out for a wing that was both clean and blocked with a piece of tape of width 0.1b positioned at mid-span and results are shown in Figure 5. Some variation with Re is seen for lift coefficient, however in percentage terms the variation is small and is substantially smaller than the difference between the clean and partially blocked results. Some change of the drag coefficient is seen at low Re but little trend with Re is seen at

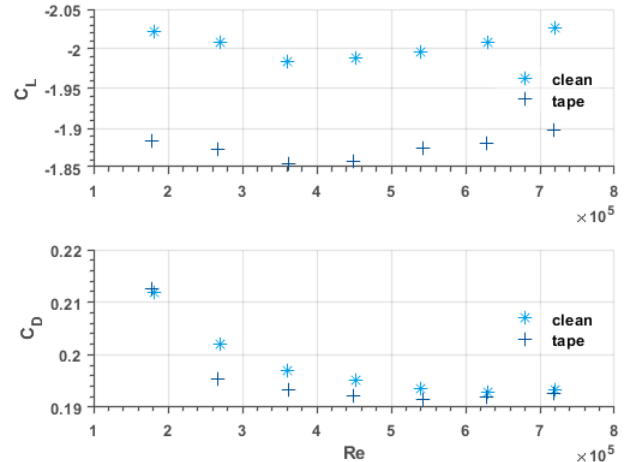the Re of 7.4 x 10^5 used in the remaining results presented in this paper.

Figure 5. Variation of lift (top) and drag (bottom) coefficients with chord based Reynolds number for high flap angle

Force Variation with Increasing Blockage Width

The effect of increasing the size of the blockage between elements was investigated experimentally by increasing the size of the taped section. The results of this on lift and drag coefficient are shown in Figure 6 for 20° flap angle. As might be expected the downforce is reduced with increasing blockage size. With the downforce reducing almost linearly to a greatest loss in downforce coefficient of ΔC_L=0.45 (or 22%) experienced when the tape blocked 80% of the slot gap. The trend with blockage size appears to intercept the zero blockage axis at a downforce coefficient of approximately 1.9 indicating that even a very thin blockage will reduce downforce due to the wake formed behind it.
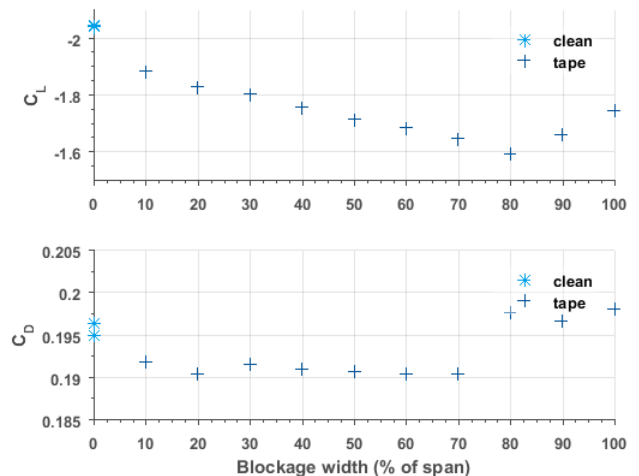

Figure 6. Variation of lift (top) and drag (bottom) coefficients with width of continuous blockage high flap angle

The introduction of the tape blockage resulted in a reduction in the drag coefficient of around ΔCD=0.003. This loss of drag remained relatively constant as the blockage width increased to 70% of the span. As the blockage was expanded to cover more than 80% of the gap both the downforce and drag increased. This suggests that when

the blockage extends towards the ends of the wing that there is some interaction between the effect of the blockage and the flow generated by the junction of the wing elements and the end plate. This suggests that the location as well as the size of the blockage will influence the loss of downforce experienced by the wing. Also the debris is more likely to block localised sections of the gap rather than continuous sections and together these motivate the next section that investigates the influence of the positioning of the blockage.

Force Variation with Blockage Position

The effect of blockage position was investigated initially by moving a single piece of tape from mid-span out towards the end plate for the high flap angle case. The effect on downforce and drag are shown in Figure 7. Introducing the 10% blockage at mid-span reduces the downforce coefficient from 2.05 to 1.88 which is consistent with the result seen in the previous section. It is interesting that introducing the blockage has reduced the drag, indicating that the drag is being reduced by removing some of the suction on the rear of the flap. As the tape is moved outwards the reduction in downforce and drag is found to be almost constant to a position around 30% of the distance to the end plate. This suggests that in this region the tape has caused the separation of a fixed area of the flap and that this causes the same change in forces wherever it is located within this region. However, at a position of 30% span from the centre line there is a step change in both downforce and drag. This is consistent with the results seen for a continuous piece of tape where increases in forces were also seen when the tape extended close to the end plate. This suggests that an interaction with the junction flows created by the end plates leads to the separation caused by the blockage having less effect when close to the end plate. However, the downforce does not increase back to the fully clean value of 2.05 while the drag slightly exceeds its clean value, indicating that there is a reduction in the performance of the wing when the blockage is in this region even if it is not as great as when a blockage is more central.
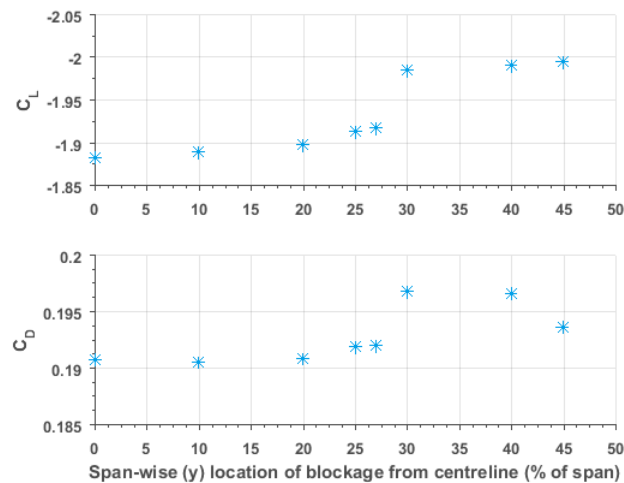

Figure 7. Variation of lift (top) and drag (bottom) coefficients with position of a single 10% span tape blockage

The effect of blockage position was then tested by using two 5% span tape sections placed symmetrically about mid span. This was done for both low and high flap angles. The results for the low flap angle are shown in Figure 8 where for this relatively lightly loaded case very little change is seen for lift or drag regardless of where the tape is positioned. Figure 9 shows the results for the high flap angle case. With the flap subject to higher loading the tape now makes significant changes to the forces on the wing. Unlike for the single

piece of tape, where the reduction in downforce was approximately constant when the tape was in the central region, the downforce reduces with increased blockage spacing to a minimum when the tapes are 35% of span apart. Again, in contrast to the single tape the downforce then increases gradually as the tapes are moved further towards the end plates.
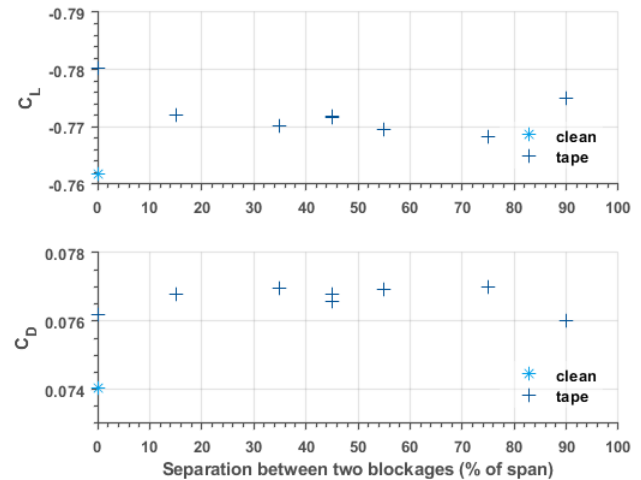

Figure 8. Variation of lift (top) and drag (bottom) coefficients with width separation of two 5% tape section for low flap angle. Note the reduced axis range in this case.

Figure 9 also presents CFD results for this case. As seen in Table 2 the CFD under predicts the downforce for the clean configuration. However, it does provide a very good prediction of the trend of both downforce and drag with tape position. In particular the downforce results all have a similar offset to the experimental data. This allows the CFD simulations to be used, together with experimental flow visualisation, to explain and further understand some of the results seen in this work.
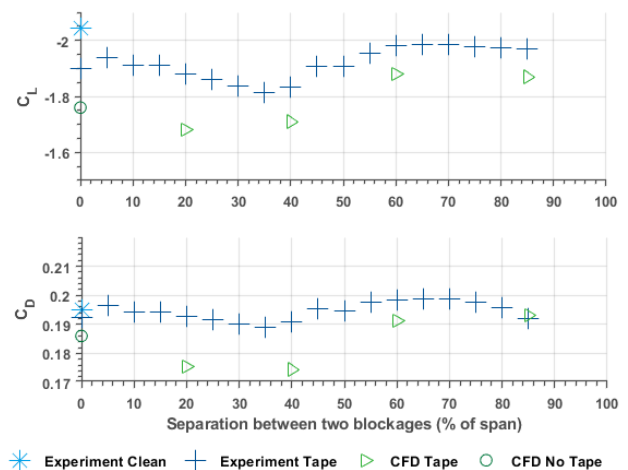

Figure 9. Variation of lift (top) and drag (bottom) coefficients with width separation of two 5% tape section for high flap angle. Results from experiment and CFD.

Flow visualisation

Figure 10 shows a comparison between experiment and CFD for the flow pattern on the false floor for high flap angle case in a clean configuration. The experimental image is a photograph showing flow visualisation paint taken after the wing is removed and the CFD image shows surface streamlines obtained from the flow vectors in the near wall cells. In both cases clear evidence can be seen that the flow is separating off the floor of the tunnel. The effect of the end plate can be seen in both as can the shape of the wake. However, the position of the separation is predicted to be in a different location to that seen in experiment. Separations and separated flow are known to be problematic for steady RANS models and the difference seen here explains at least some of the difference seen between experimental and CFD forces even for a 'clean' condition. For future work it may be necessary to use low y+ modelling even for the tunnel floor or potentially eddy resolving methods such as DES.
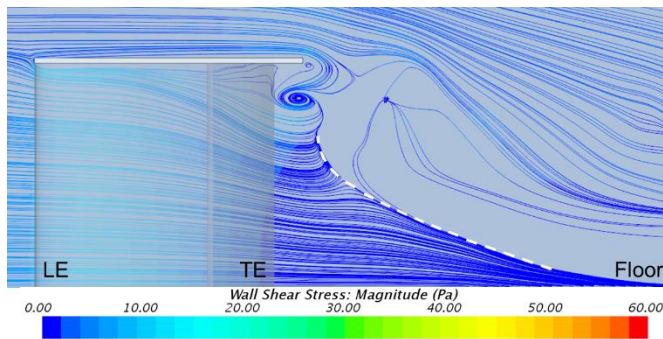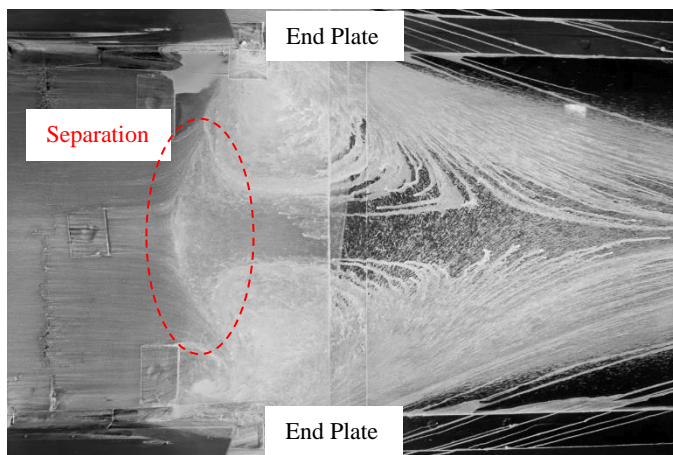

Figure 10. Flow pattern on tunnel false floor from experiment (top) and CFD (bottom) for clean wing assembly with high flap angle. Experimental image shows flow visualization paint and CFD image shows surface streamlines.

CFD surface streamlines on the underside of the wing are shown for two different tape spacings in Figure 11. These spacings are 20% span, where the downforce is decreasing with increased spacing, and 60% span where the downforce has increased. The CFD was carried out using a symmetrical domain and so another blockage is notionally located equidistant from the centre line. The information contained in these images can be used to explain some of the trends seen in the force measurements. A region of separated flow can be seen on the flap behind the tape that is responsible for the reduction in both downforce and drag on this element. The separation can be seen to diverge outwards from the tape, which explains why for the case with two blockages the downforce reduction increases as the gap moves from 0 to 30% span. With a small gap, the two separation regions will overlap and the total separated area will increase as the gap

increases. The gap in Figure 11a is 20% and the inboard edge of the separation can be seen to intercept the centre line meaning that there is still some overlap between separations at this spacing. This is consistent with Figure 9 where it can be seen that the minimum downforce, corresponding with maximum separated area, is obtained for a gap slightly larger than 20%. The reduced effect on downforce when the gap is moved close to the end plates is explained by Figure 11b. For a tape separation of 20%, the region of separation behind the debris spreads equally on each side. The wake from each tape spans approximately 25% of the wing-span at the trailing edge of the flap. Conversely, for a debris separation of 60%, the wake is much narrower on the side closest to the endplate. This is due to the secondary flows induced by the presence of the endplate that can be seen to cause the flow to move inboard on the main element. This would reduce the size of the separated region between the debris and the endplate and therefore lead to a smaller loss of downforce.
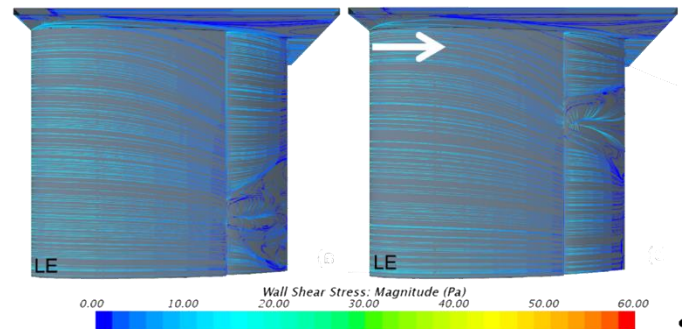

Figure 11. CFD surface streamlines on the underside of the main element and flap for the high flap case. Only half of the span of the wing is shown. Tape separation is 20% in the left image and 60% in the right image of the total wing span.

Comparison to On-Road Conditions

As the experiments were run using a wind tunnel with a stationary ground plane the results would not be expected to correspond to those found on-road. The CFD can be used to artificially introduce a moving ground plane and remove the presence of the tunnel walls and roof, as described in the CFD methodology section. The results of doing this are shown in Figure 12 for the high flap angle case with two tape blockages with variable spacing. Also shown for reference are the experimental and CFD results for the stationary ground tests. The downforce is seen to reduce for all blockage spacings compared to the tunnel results. The trend with spacing is very similar to tunnel conditions but the change in downforce is reduced. The drag is also seen to vary less with tape spacing with a moving ground plane. This indicates, as is also shown experimentally in Figure 8, that debris has a greater effect on the performance of wing that is more highly loaded in its clean configuration. While the effect of debris appears to reduce for on-road conditions, it is likely that a racing car wing would be designed to be as highly loaded as possible. Therefore, changes in downforce similar to, or even greater than, those seen for the tunnel conditions could be encountered in the presence of debris.
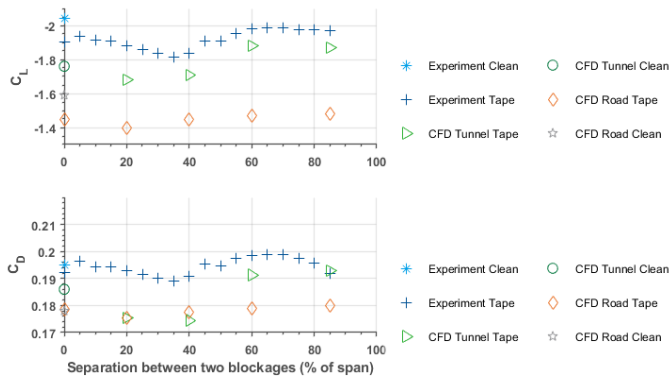
Figure 12. Variation of lift (top) and drag (bottom) coefficients with width of separation of two 5% tape section for high flap angle. Results are from CFD at tunnel and 'on-road' conditions. Tunnel condition results from experiment also shown for reference.

Conclusions

The influence of a blockage of the gap between main element and flap of a two-element wing in ground effect has been investigated. This was performed experimentally using lengths of tape to seal the gap and comparing downforce and drag to the clean configuration. Increasing the length of a central blockage was seen the decrease the downforce almost linearly with a minimum downforce coefficient of 1.6 found with an 80% blockage compared to a clean coefficient of 2.05. When the blocked section was increased beyond 80% of span the downforce was seen to increase slightly. This was then investigated further by changing the position of a fixed length of tape. It was seen that a single 10% span blockage caused a reduction in downforce coefficient compared to the clean wing of approximately 0.15 when positioned anywhere between the centerline and mid-way between centerline and the end plate. This single blockage is more representative of a large piece of debris and suggests that significant losses of downforce could be caused by on-track debris. When the blockage was moved further towards the end plate the downforce was seen to increase again. This reduced effect of the blockage when close to the endplates is also seen for a case where two blockages are placed symmetrically either side of the centerline. In this case the downforce is seen to reduce with increased separation until about 40% of span where it again increases. CFD simulations of this case were seen to reproduce the trends but with reduced downforce values for all spacings. This indicates the difficulty steady RANS methods have in accurately predicting separated flows as seen in this kind of flow. The effect of debris on the wing's performance was seen to be increased when the loading on the clean wing is increased. This highlights the importance of considering the influence that debris could have on a wing that has been designed to maximise downforce. Results from the CFD show that there is a separated region that forms a 'V' shape on the suction side of the flap spreading out from the blockage. As the two blockages are moved further apart the amount of overlap between the two separations is reduced and the total separated area increases, this explains why the downforce reduces with greater distance between the blockages. However, when the blockage moves close to the end plate the secondary flows from the junction of the wing and the endplate cause the separated regions to be reduced in size, which explains the reduced effect on downforce seen when the blockage approaches the endplates.

References

[1]   J. Katz, Race Car Aerodynamics - Designing for Speed, Cambridge, Massachusetts: Bentley Publishers, 2006.

[2]   J. Zerihan and X. Zhang, "Aerodynamics of a Single Element Aerofoil in Ground Effect," *Journal of Aircraft,* vol. 37, no. 6, pp. 1058-1064, 2000.

[3]   R. Ranzenbach and J. B. Barlow, "Two-Dimensional Airfoil in Ground Effect, An Experimental and Computational Study," *Society of Automotive Engineers, Paper 942509,* pp. 241-249, 1994.

[4]   K. Knowles, D. Donahue and M. Finnis, "A Study of Wings in Ground Effect," in *Loughborough University Conference on Vehicle Aerodynamics, The Royal Aeronautical Society*, London, UK, July 1994.

[5]   W. J. Jasinski and M. S. Selig, "Experimental Study of Open-Wheel Race-Car Front Wings," *Society of Automotive Engineers, Paper 983042,* November 1998.

[6]   M. Soso and P. Wilson, "Investigating Changes to the Downforce Curve of a Double Element Airfoil in Ground Effect," *Society of Automotive Engineers, Paper 2004-01-3558,* November 2004.

[7]   X. Zhang and J. Zerihan, "Aerodynamics of a Double-Element Wing in Ground Effect," *American Institue of Aeronautics and Astronautics,* vol. 41, no. 6, pp. 1007-1015, June 2003.

[8]   X. Zhang and J. Zerihan, "Edge Vortices of a Double-Element Wing in Ground Effect," *Journal of Aircraft,* vol. 41, no. 5, pp. 1127-1137, September 2004.

[9]   S. Mahon and X. Zhang, "Computational Analysis of a Inverted Double-Element Airfoil in Ground Effect," *American Society of Mechanical Engineers,* vol. 128, pp. 1172-1180, November 2006.

[10] M. B. Bragg, A. P. Broeren and L. A. Blumenthal, "Iced-Airfoil Aerodynamics," *Progess in Aerospace Sciences,* vol. 41, no. 5, July 2005.

[11] W. Sang, F. Li and Y. Shi, "Icing Effect Study for Wing/Body and High-Lift Wing Configurations," in *45th AIAA Aerospace Sciences Meeting and Exhibit*, Nevada, 2007.

[12] C. Bidwell, "Icing Calculations for a 3D, High-Lift Wing Configuration," in *43rd AIAA Aerospace Sciences Meeting and Exhibit*, Nevada, 2005.

[13] D. Silva, T. Bortholin, J. Lyrio and L. Santos, "Parametric Evaluation of Icing Effects by a Quasi-3D Methodology for High-Lift Configurations, Paper 2015-01-2083," in *SAE 2015 International Conference on Icing of Aircraft, Engines and Structures*, 2015.

[14] D. M. Silva and L. G. Trapp, "Improving Ice Accretion Simulation Through the use of CFD," *Society of Automotive Engineers, Paper 2011-38-0054,* 2011.

[15] G. Johl, M. A. Passmore and P. M. Render, "Design methodology and performance of an indraft wind tunnel," *The Aeronautical Journal,* vol. 1087, no. 108, pp. 465-473, 2004.

[16] CD-adapco, "STAR-CCM+ V11," 2016.

Contact Information

Emma Corfield

Andrew Garmory
a.garmory@lboro.ac.uk

Graham Hodgson
g.hodgson@lboro.ac.uk

Acknowledgments